Development/Plasticity/Repair

Functional and Anatomical Reorganization of the Sensory-Motor Cortex after Incomplete Spinal Cord Injury in Adult Rats

Arko Ghosh,[1] Esther Sydekum,[2] Florent Haiss,[3] Stefano Peduzzi,[1] Björn Zörner,[1] Regula Schneider,[1] Christof Baltes,[2] Markus Rudin,[2,3] Bruno Weber,[3] and Martin E. Schwab[1]

[1]Brain Research Institute and [2]Institute for Biomedical Engineering, University of Zurich and Swiss Federal Institute of Technology Zurich, 8057 Zurich, Switzerland, and [3]Institute of Pharmacology and Toxicology, University of Zurich, 8057 Zurich, Switzerland

A lateral hemisection injury of the cervical spinal cord results in Brown-Séquard syndrome in humans and rats. The hands/forelimbs on the injured side are rendered permanently impaired, but the legs/hindlimbs recover locomotor functions. This is accompanied by increased use of the forelimb on the uninjured side. Nothing is known about the cortical circuits that correspond to these behavioral adaptations. In this study, on adult rats with cervical spinal cord lateral hemisection lesions (at segment C3/4), we explored the sensory representation and corticospinal projection of the intact (ipsilesional) cortex. Using blood oxygenation level-dependent functional magnetic resonance imaging and voltage-sensitive dye (VSD) imaging, we found that the cortex develops an enhanced representation of the unimpaired forepaw by 12 weeks after injury. VSD imaging also revealed the cortical spatio-temporal dynamics in response to electrical stimulation of the ipsilateral forepaw or hindpaw. Interestingly, stimulation of the ipsilesional hindpaw at 12 weeks showed a distinct activation of the hindlimb area in the intact, ipsilateral cortex, probably via the injury-spared spinothalamic pathway. Anterograde tracing of corticospinal axons from the intact cortex showed sprouting to recross the midline, innervating the spinal segments below the injury in both cervical and lumbar segments. Retrograde tracing of these midline-crossing axons from the cervical spinal cord (at segment C6/7) revealed the formation of a new ipsilateral forelimb representation in the cortex. Our results demonstrate profound reorganizations of the intact sensory-motor cortex after unilateral spinal cord injury. These changes may contribute to the behavioral adaptations, notably for the recovery of the ipsilesional hindlimb.

Introduction

High cervical unilateral hemisection injuries result in the Brown-Séquard syndrome in humans (Brown-Séquard, 1868). In this injury, one-half of the spinal cord is completely spared; limbs on this contralesional side are able to perform their motor functions and are overused (Tattersall and Turner, 2000). These intact side limbs are, however, insensitive to pain and temperature because of the interrupted crossed spinothalamic tract. Ipsilesional limbs are severely dysfunctional without mechanoception and proprioception, but they retain their perception of pain and temperature. Interestingly, significant functional recovery of crude movements, especially of the legs, enables the patients to walk with minimal support (Taylor and Gleave, 1957; Little and Halar, 1985). The adaptations of the sensory-motor cortex that accompany the overuse of contralesional limbs and the recovery of the ipsilesional leg remain unknown.

The adult sensory-motor cortex can undergo dramatic reorganizations after spinal cord injury in rats and humans (Raineteau and Schwab, 2001; Kaas et al., 2008). After thoracic injuries, the hand/forelimb representation expands; the expanded territory includes the denervated leg/hindlimb cortex in humans and rats (Bruehlmeier et al., 1998; Endo et al., 2007). To address the adaptations after unilateral spinal cord hemisection injury, we focused on the intact (ipsilesional) sensory-motor cortex of adult rats. The intact cortex may participate in the spontaneous behavioral recovery of the ipsilesional hindlimb; it is not known whether the spared corticospinal tract (CST) spontaneously sprouts across the midline to innervate the denervated half of the spinal cord. Unilateral cortical injury or pyramidotomy also deprives the spinal cord unilaterally of direct cortical input. In adult rodents, sprouting of the CST from the intact side across the midline can be induced by suppression of the neurite growth inhibitor Nogo pathway (Thallmair et al., 1998; Wiessner et al., 2003), by local neurotrophic factors (Zhou and Shine, 2003), or by electrical stimulation of the injury-spared CST (Brus-Ramer et al., 2007). The rearranged CST is crucial for the observed recovery of skilled movements (Kartje-Tillotson et al., 1987).

Received April 16, 2009; revised Aug. 20, 2009; accepted Aug. 20, 2009.

This work was supported by the Swiss National Science Foundation (Grants 31-63633.00 and 31-122527); the National Center of Competence in Research "Neural Plasticity and Repair" of the Swiss National Science Foundation; the Spinal Cord Consortium of the Christopher Reeve Paralysis Foundation (Springfield, NJ); and NeuroNe, Network of Excellence of the European Consortium for Research in Neurodegenerative Diseases (Sixth Framework European Union Program). We are grateful to Eva Hochreutener, Miriam Gullo, Jeannette Scholl, Roland Schoeb, Martina Röthlisberger, and Lisa Schnell for technical assistance. We thank Anita Buchli, Thomas Mueggler, Vincent Pernet, and Michelle Starkey for helpful discussions.

Correspondence should be addressed to Arko Ghosh, Institute of Neuroinformatics, Swiss Federal Institute of Technology Zurich and University of Zurich, Winterthurerstrasse 190, 8057 Zurich, Switzerland. E-mail: arko@ini.phys.ethz.ch.

DOI:10.1523/JNEUROSCI.1828-09.2009

 0270-6474/09/2912210-10$15.00/0

Using blood oxygenation level-dependent functional magnetic resonance imaging (BOLD-fMRI), voltage-sensitive dye (VSD) imaging, and anatomical tract tracings of the intact cortex, we addressed the reorganizations that accompany the forelimb overuse and the hindlimb recovery in the Brown-Séquard rat. Adult rats were unilaterally transected at cervical segments (C3/4). BOLD-fMRI and VSD experiments showed an enhanced representation of the unimpaired forelimb in the corresponding sensory cortex. Anterograde tracing of the intact side CST showed midline-crossing neurons in both cervical and lumbar segments. Retrograde labeling of the midline-crossing CST from the cervical segments (C6/7) reflected a somatotpic organization of the axons undergoing structural rearrangement. The highly sensitive VSD imaging showed specific but delayed activation of the intact, ipsilesional sensory-motor cortex after stimulation of the injury-affected hindpaw. This suggests that the new ipsilateral corticospinal projection has access to ipsilesional hindpaw sensory input and compensates, in part, for the lost contralateral motor and sensory connections.

Materials and Methods

Experimental subjects. Adult female Lewis rats (200–220 g; obtained from R. Janvier, Le Genest-St Isle, France) were used in this study. Animals were housed in groups of four in standardized cages (type 4 Macrolon) at a 12 h light/dark cycle with food and water *ad libitum*. All animals were given 1 week to acclimatize to their housing before experimentation. All experimental procedures performed were in adherence to the guidelines of the Veterinary Office of the Canton of Zurich, Switzerland.

Spinal cord injury. Spinal cord lateral hemisection injuries were performed in rats deeply anesthetized with a subcutaneous injection of Hypnorm (120 μl/200 g body weight; VetaPharma) and Dormicum (0.75 mg in 150 μl/200 g body weight; Roche Pharmaceuticals). Vertebral segment C4 (corresponding to spinal segment C3/4) was identified by counting of vertebral spines from segment T2. A dorsal unilateral laminectomy was performed at C4 to expose the dura-covered spinal cord. The dura was removed using blunt iridectomy scissors and a fine forceps. Using sharp iridectomy scissors, a lateral spinal cord hemisection was performed. To ensure a complete hemisection, a 36G needle was inserted at the midline to scrape the vertebra along the lesion. After surgery, animals were administered an analgesic (2.5 mg per subcutaneous injection of Rimadyl; Pfizer) once per day for 5 d and antibiotics (1.25 mg/250 g body weight intraparetonium injection of Baytril; Bayer) once per day for 3 d. Bladders were checked and emptied three times per day until their function had completely recovered. Spinal cord injuries were histologically verified postmortem. Incompletely injured or overhemisected rats were subsequently eliminated from analysis.

Behavioral data acquisition and analysis. Behavioral tests were performed on the catwalk and horizontal ladder. Before injury, animals were exposed to the behavioral tests four times (for each test, both tests were conducted on the same day). Three exposures spread over 2 weeks were followed by acquisition of baseline measurements. Each exposure (before the baseline measurements) involved three to five attempts on the behavioral tests.

The catwalk analysis system has been described previously in detail (Hamers et al., 2006). Briefly, this system consists of a glass runway, with customized lighting, which is video recorded as the animals traverse the runway. From these videos, the system determines the percentage of usage by each paw and the intensity of footprints during maximum paw contact at every step.

The horizontal ladder consisted of equally spaced (at 6 cm gaps) rungs. The ladder was 1 m long and elevated at 1 m. Three trials were video recorded over a 60 cm stretch. Videos were analyzed off-line. Similar to the original description of the method (Metz and Whishaw, 2002), steps that resulted in the paw being placed such that the limb did not slip from the rung (weight-supported steps) were noted as successful. In our analysis, when a correction led to a weight-bearing step on a rung, we considered it as a successful step. Therefore, a successful step reported here includes the categories of correction, partial placement, and correct placement described previously (Metz and Whishaw, 2002). The percentage of successful steps of an animal was determined by averaging over three trials. When an attempted placement failed to make contact with the ladder rung, it was noted as missed. In the missed placement analysis, only the first attempted placement on a rung and not the corrected placements were considered.

BOLD-fMRI. Rats were scanned before and after injury on a Biospec 94/20 horizontal bore small animal MRI system (BGA-12 gradient system; gradient strength, 400 mT/m; Bruker BioSpin MRI) under isoflurane anesthesia (1.5%) and a muscle relaxant (3 mg/200 g body weight Gallamine; Sigma-Aldrich). Anatomical images were obtained using the multislice rapid acquisition with relaxation enhancement (RARE) spin echo sequence [parameters: field of view (FOV), 53×25 mm^2; matrix dimension (MD), 256×128; slice thickness (SLTH), 1 mm; interslice distance (ISD), 1.25 mm; echo delay , 60 ms; repetition delay , 1259 ms; RARE factor, 8; number of acquisitions, 1; acquisition time (T_{acq}), 1.25 min]. Functional MRI data based on the BOLD signals were recorded using a serial gradient-echo echo planar imaging (EPI) sequence (FOV, 33×25 mm^2; MD, 64×64; SLTH, 1 mm; ISD, 1 mm; T_{acq}, 10 s; 50 repetitions). To cover all cortical layers, two adjacent horizontal slices were acquired. Both forepaws (in six rats, before and after injury) and the hindpaw (in four intact rats) were stimulated using needle electrodes. Stimulation parameters for the forepaws were as follows: amplitude, 6 mA; pulse duration, 0.5 ms; frequency, 3 Hz. A repetitive block design has been used with five on periods of 40 s and five off periods of 60 s each. Hindpaws were stimulated using a similar stimulation, but at 1.5 mA.

Data were analyzed using the Biomap software (version 4; M. Rausch, Novartis) with statistical processing based on the general linear model approach. Thresholds for considering activation were $p < 0.01$ and a minimum area of five voxels. The method used to create BOLD maps incorporating data from different animals was described in detail previously (Sydekum et al., 2009). Briefly, the data of the individual animals were spatially normalized using anatomical landmarks identified on the EPI images (using custom-written, IDL-based software; RSI). Subsequently, maximum intensity projections of the two horizontal sections were calculated for each animal and added up to yield an overlapping activation map (using another custom-written MATLAB-based program; MathWorks).

Optical imaging of the cortex using a VSD. Optical imaging using the VSD RH1691 was performed as documented previously, with some alterations (Ferezou et al., 2007), under isoflurane anesthesia (4% for induction, maintained at 1.5% during imaging, 3% while not imaging). The sensory-motor cortex was exposed carefully, and the VSD was topically added; the dye was dissolved 1 mg/ml Ringer's solution containing the following (in mM): 135 NaCl, 5 KCl, 5 HEPES, 1.8 $CaCl_2$, and 1 $MgCl_2$. The dye was allowed to diffuse on the cortical surface and deeper for 1 h. Unbound dye was washed from the surface using Ringer's solution. The cortex was then covered with 2% agar solution and with a glass coverslip. Under shutter control, VSD was excited with 630 nm light from a 150 W halogen lamp (Karl Storz). A 650 nm dichroic mirror was used to reflect the excitation light. Excitation light was focused on the cortical surface using a camera lens (50 mm f/1.4; Canon). The emitted light was collected using the same optical pathway, passing the dichroic, long pass filtered (665 nm), and focused onto the sensor of the high-speed CMOS camera (Micam Ultima; Scimedia) via another identical 50 mm lens. Images were acquired using a 14 bit/pixel 100×100 recording array and covered a 6×6 mm FOV with a 5 ms temporal resolution. Analyses were based on bleach corrected averages of 10 trials. Bleach correction (double-exponential fit), conversion to changes in VSD fluorescence intensity ($\Delta F/F_0$%) and region-of-interest (ROI) analyses were performed using PMOD (PMOD Technologies). Animals were stimulated (subcutaneous forepaw or hindpaw) with a single pulse (600 μA amplitude, 1 ms duration). Unlike in the previous description of the method (performed in mice), there was no need to synchronize the recording to electrocardiogram to obtain robust and reproducible signals.

Anterograde tracing with biotinylated dextran amine and quantification of midline-crossing axons. Intact rats or injured rats 4 weeks after lateral hemisection were anterogradely traced from the sensory-motor cortex

under isoflurane (3%) anesthesia. A total of 3 μl of biotinylated dextran amine (BDA) solution [10,000 MW; 10% in 0.1 M phosphate buffer (PB); Invitrogen] was injected using a 34 gauge Nanofil syringe (WPI). Twenty-one days after the injections, animals were overdosed with Nembutal and perfused with a fixative, 400 ml of Ringer's solution containing 4% paraformaldehyde and 5% sucrose. Spinal cords and brains were immediately removed and postfixed overnight in the same solution. The tissue was immersed in 30% sucrose before being frozen, cross sectioned (40 μm thick at 120 μm gaps), and collected on a glass slide. BDA was visualized using an ABC Elite kit (Vector Laboratories) and nickel-intensified DAB reaction.

Camera lucida drawings of midline-crossing axons were visualized by overlapping traces of four consecutive sections. Innervation maps were generated from the points at which midline-crossing axons crossed intersections (final magnification, 400×; Neurolucida 7.0; MicroBrightField), on an equally spaced vertical line grid covering the ipsilateral spinal cord gray matter (spacing of 80 μm, with two additional lines spaced at 50 μm before and after the midline). The acquired data from 40 consecutive cervical (C5–C8) and lumbar (L2–L6) sections were processed with a custom-written MATLAB (MathWorks) program that incorporated the preexisting scattercloud function (MATLAB Central; MathWorks). For quantification of midline-crossing CST axons, the total number of intersections was evaluated on three vertical lines in cervical and lumbar segments (M, D1, and D2) (see Fig. 2). These counts were corrected for variability in dye uptake by normalizing with a measure that reflects the density of labeled CST in the dorsal funiculus; dividing the number of midline-crossing CST fibers with the product of m/A, where m is the mean axonal counts from three different ROIs in the dorsal funiculus sampled from a cervical or lumbar section and A is the area of labeled CST.

Retrograde tracing and labeled cell analysis. Rats were fixed on a modified stereotaxic frame under deep anesthesia (Hypnorm and Dormicum as mentioned above): the head was fixed using ear bars, and the cervical vertebra was fixed using clamps placed on either side of the vertebral column. A unilateral laminectomy was performed at C6 and C7, and the dura was removed. Using a 28 gauge Nanofil syringe attached to a UltraMicroPump (WPI) mounted on the stereotaxic frame, 1% Fast Blue (EMS-Polyloy) suspension in 0.1 M PB and 2% DMSO was injected into the spinal cord. Each animal had five injections of 120 nl of Fast Blue spaced at ~0.5 mm, along the spinal cord. The coordinates for injections were 0.75 mm lateral from the midline and 1.2 mm below the spinal cord surface. Unilaterality of the injection was verified postmortem. Ten days after injection, animals were perfused and processed for cryosectioning as mentioned above. Series of 50 μm brain cross sections (with 100 μm gaps) were used for quantification of labeled cells

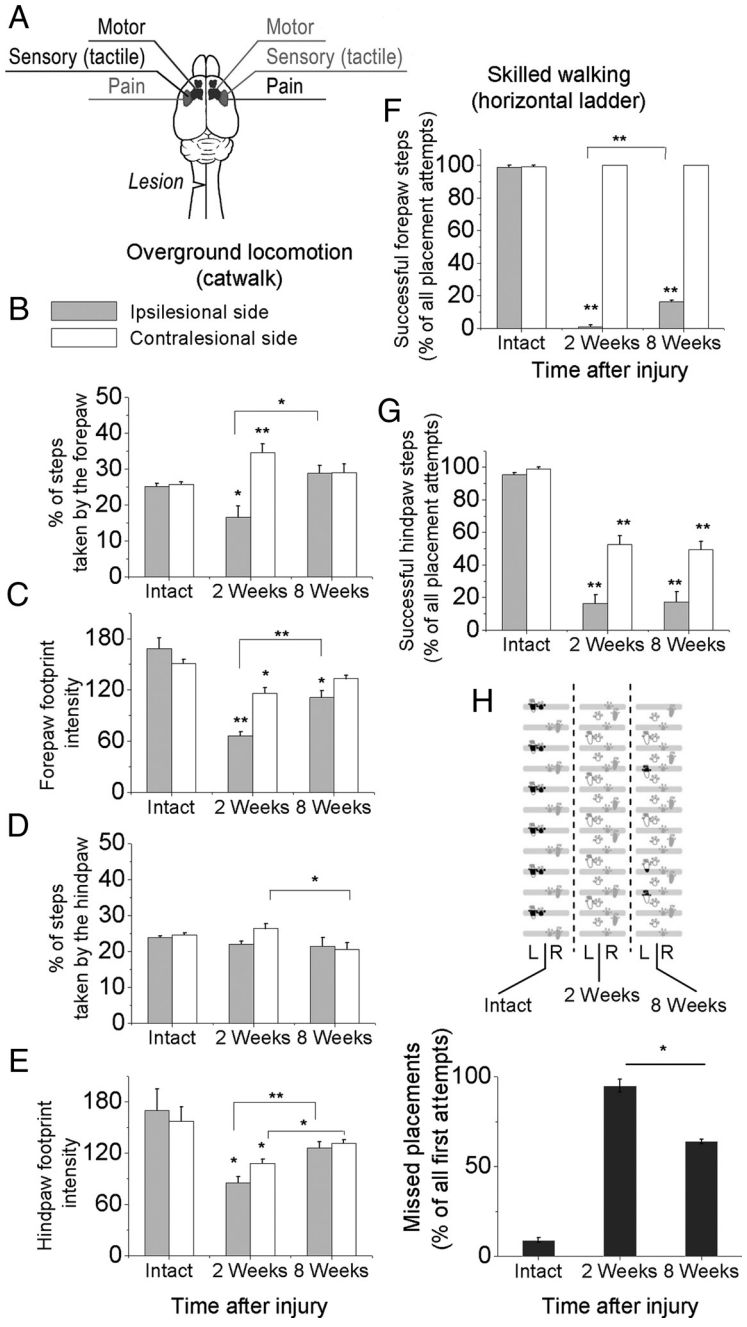

Figure 1. Significant recovery of overground locomotion and poor recovery of skilled movements by the ipsilesional limbs after lateral hemisection of the cervical (C3/4) spinal cord. ***A***, Schematic view of the injury model used that leads to Brown-Séquard syndrome. Text in gray denotes absence and text in black denotes presence of input or output after the injury. ***B–E***, While walking on a flat runway (catwalk), animals altered their walking pattern to increase their use of the contralesional forelimb at 2 weeks. ***B***, At 8 weeks, the walking pattern recovered to normal. ***C***, Body weight support (loading of limb, footprint intensity) for the ipsilesional forepaw showed a 2.5-fold decrease 2 weeks after injury to recover significantly by 8 weeks. ***D***, Hindpaw rhythm after injury remained similar to preinjury baseline. ***E***, The ipsilesional hindpaw also showed a decrease in footprint intensity at 2 weeks and a consecutive recovery 12 weeks after injury. ***F***, ***G***, Skilled movements, as required while walking on a horizontal ladder, remained severely and permanently affected after injury. ***F***, The ipsilesional forepaw was unable to successfully step on the ladder after injury and showed no recovery over 8 weeks. ***G***, The ipsilesional hindpaw was similarly affected and did not show any recovery in the number of functional placements. ***H***, A schematic view of the first placement attempts on a ladder rung, drawn based on a rat before and after injury. L, Left (ipsilesional) forepaw and hindpaw; R, right (contralesional) forepaw and hindpaw (in gray). Horizontal ladder rungs are in gray. The area of ipsilesional paw contacts on the horizontal ladder is in black. Notably, the ipsilesional hindpaw showed significant recovery after 8 weeks in the number of attempted steps that made contact with the ladder rung and thus resulted in a decreased number of missed placements. $n = 6$ rats ($n = 5$ for ***H***), ±SEM. Data were subjected to the nonparametric Mann–Whitney U test. *$p < 0.05$; **$p < 0.01$. Where not indicated, statistics are compared with the respective data in intact animals.

and for reconstruction of corticospinal representation using Neurolucida (MBF Bioscience). In four separate animals, the retrograde tracer Fast Blue (3 μl) was applied into the cut CST in thoracic segment 8 to determine the hindlimb CST representation in the cortex.

Results

Locomotion deficits and recovery after a C3/4 lateral spinal cord hemisection

To assess the functional consequence of a unilateral hemisection injury (Fig. 1*A*; supplemental Fig. 1, available at www.jneurosci.org as supplemental material), adult rats were tested on an automated footprint analysis system, on the catwalk, and on a horizontal ladder. The catwalk measurements were taken while the animal walked on a flat runway, which requires little skill in contrast to the grips and placements required for crossing a horizontal ladder (Metz and Whishaw, 2002; Bolton et al., 2006). All animals ($n = 6$) were trained on the behavioral tests, and baseline measurements were obtained before injury. Immediately after injury, the rats displayed a flaccid paralysis of the ipsilesional forelimbs, whereas the hindlimbs appeared spastic. This lasted for no >5 d. One week after injury, the ipsilesional forelimb remained unused, and the fist remained closed, whereas the hindlimb regained its ability to step. In the first 2 weeks, animals often lost their balance while walking in their home cages. When placed on a flat surface 2 weeks after injury, for catwalk measurements, animals appeared balanced while walking. At this time point, the contralesional forepaw was used in preference to the ipsilesional forepaw (Fig. 1*B*). When the ipsilesional forepaw was placed, the amount of body weight supported by it was low, resulting in a 2.5-fold decrease in intensity of the footprint on the catwalk (Fig. 1*C*). Eight weeks after injury, the ipsilesional forepaw was used as much as the contralesional forepaw; however, the intensity of the footprint was still less than in intact animals. Although the contralesional hindpaw was not used in preference to the ipsilesional paw (Fig. 1*D*), 2 weeks after injury the body weight supported by the ipsilesional hindpaw was much lower than in intact animals (Fig. 1*E*). By 8 weeks, the footprint intensity recovered significantly (Fig. 1*E*).

While crossing the horizontal ladder, the forepaw of intact animals always gripped the ladder rungs, and the hindpaw was placed correctly at all times (described as successful steps in Fig. 1*F*,*G*). Two weeks after injury, rats could cross the horizontal ladder, but with great difficulty. The ipsilesional forepaw was rarely placed on the ladder, and if it was placed, it often slipped, resulting in a low percentage of successful steps (Fig. 1*F*). Animals, however, never fell from the ladder because of the weight-bearing step of the contralesional forepaw. At 8 weeks after injury, the animals appeared more stable on the ladder. However, the ipsilesional forepaw continued to be unable to target and grasp the ladder rungs. The ipsilesional hindpaw showed major deficits during the ladder walk (Fig. 1*G*). The contralesional hindpaw also showed deficits on the ladder. In contrast to the ipsilesional hindpaw that slipped frequently even when the paw was placed on the ladder, the contralesional hindpaw was always able to support the body weight, resulting in a higher percentage of successful steps than the ipsilesional hindpaw. We also evaluated the target precision of the ipsilesional limbs on their first placement attempt on every ladder rung. We noted the number of incidences in which the limbs made contact with the ladder rung. Interestingly, the ipsilesional hindpaw was able to improve its success rate in targeting the ladder rungs by 8 weeks after injury (Fig. 1*H*). At 2 weeks after injury, 95% of placement attempts did not result in any contact with the ladder rung, and this reduced to 64% of the steps by 8 weeks. The ipsilesional forelimb showed no improvement with this regard; the percentage of missed placements remained above 90% even at 8 weeks after injury (supplemental Fig. 2, available at www.jneurosci.org as supplemental material).

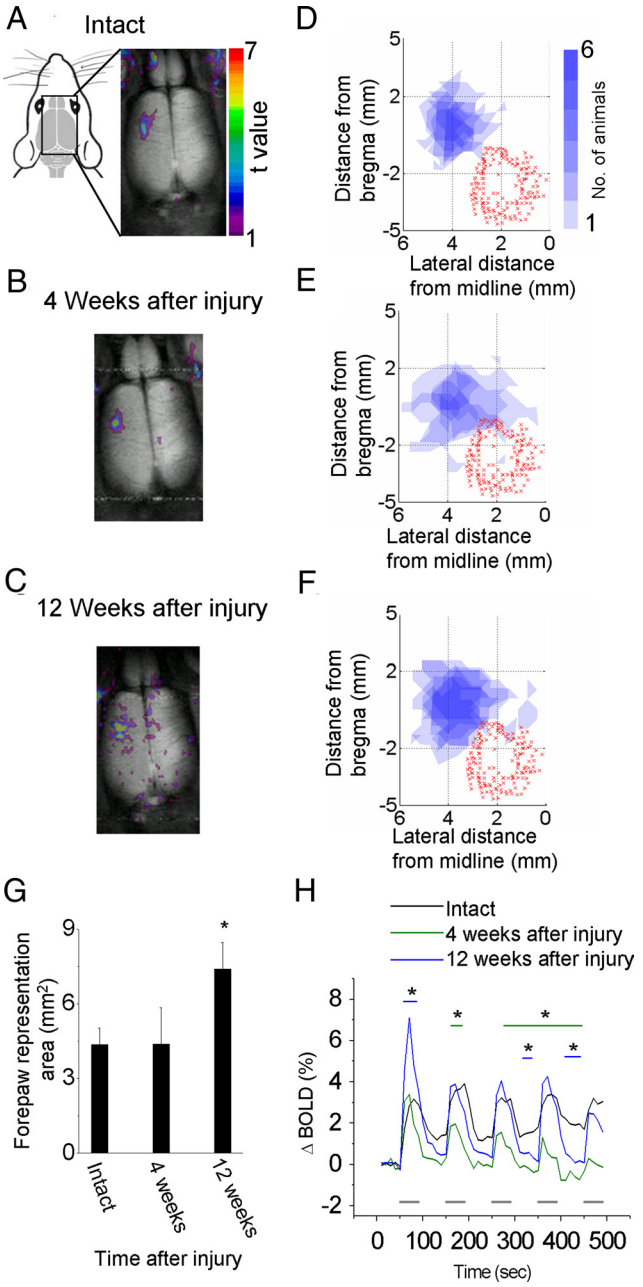

Figure 2. BOLD-fMRI reveals expansion of contralesional, unimpaired forepaw representation in the sensory-motor cortex after injury. ***A–C***, BOLD response activation maps after electrical stimulation of the contralesional forepaw before injury (***A***), 4 weeks after injury (***B***), and 12 weeks after injury (***C***). ***D–F***, Superimposed individual activation maps from intact animals (***D***), 4 weeks (***E***), and 12 weeks (***F***) after injury. The blue area represents the forepaw ($n = 6$ rats; the intensity of the color representing the number of rats displaying activation at a specific location), and red crosses show the borders of the hindpaw area in intact animals ($n = 4$ rats). ***G***, Area of forepaw representation from BOLD-fMRI maps. ***H***, Average BOLD signal change ($n = 6$ rats) after repeated forepaw stimulations (gray lines depict stimulus trains) reveals an increased amplitude 12 weeks after injury (ROI, original forepaw area) in response to the first stimulation train. The color of the line below the asterisk depicts the group to which the intact response curve was compared with. Statistics are as in the previous figure.

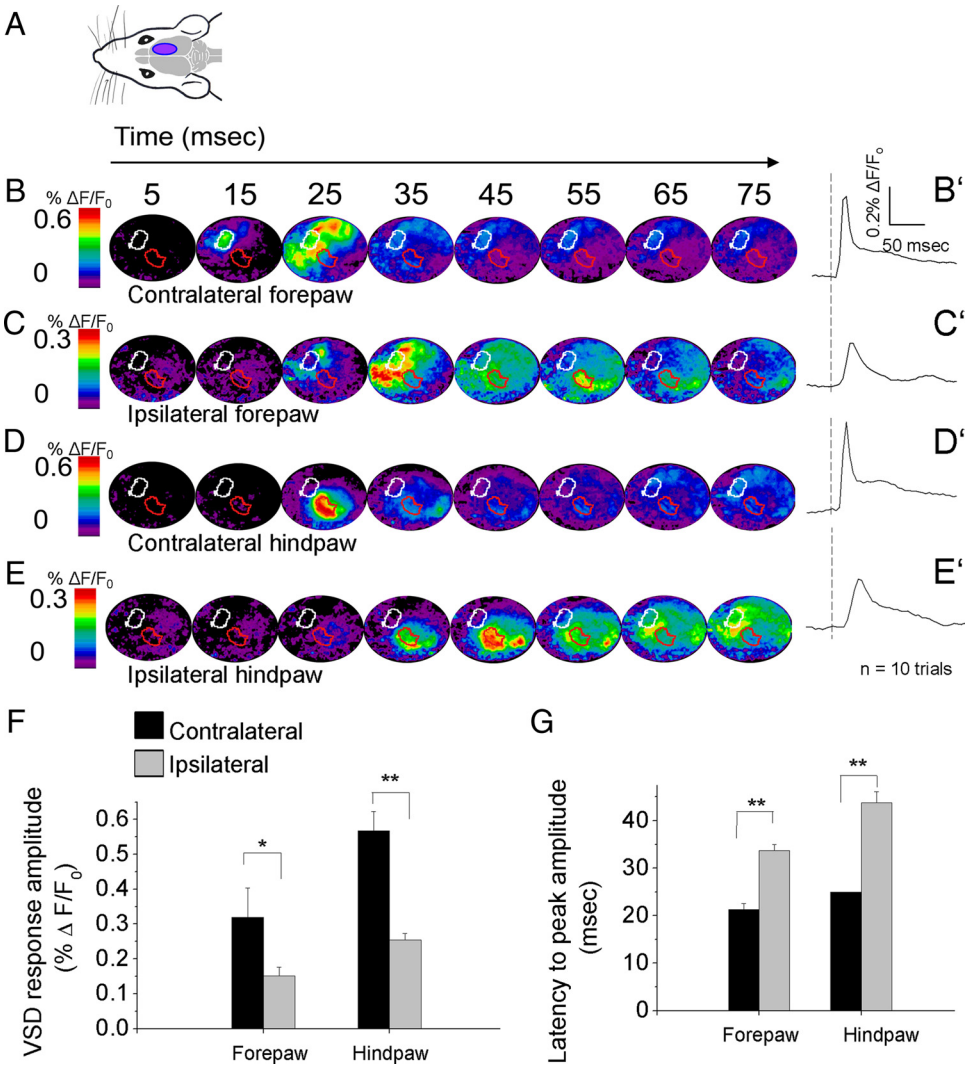

Figure 3. VSD imaging after bilateral forepaw and hindpaw electrical stimulations in uninjured animals. ***A***, Schematic view of the imaged cortical location. ***B–E***, Spatio-temporal dynamics of cortical responses after contralateral forepaw (***B***), ipsilateral forepaw (***C***), contralateral hindpaw (***D***), and ipsilateral hindpaw (***E***) electrical stimulation (600 μA single pulse; $n = 10$ trials) in an intact animal. White and red borders indicate 55% isocentric contours after forepaw stimulation (at 15 ms after stimulation) and hindpaw stimulation (at 20 ms after stimulation), respectively. ***B′–E′***, Time activity curves of the corresponding images (with ROI based on 55% isocentric contours 5 ms after the signal appears in the cortex). The vertical dashed line depicts stimulation. ***F***, ***G***, The mean peak response amplitude (***F***) and latency to peak (***G***) are also shown. Note the different color scale used in ***B*** and ***D*** compared with ***C*** and ***E***. $n = 5$ rats. Statistics are as in previous figures.

Changes in sensory representation of the forepaws in the cortex revealed using BOLD-fMRI

The injury used in this study interrupts all ascending tactile and proprioceptive sensations, but pain and temperature sensations from the ipsilesional side should remain intact. BOLD-fMRI allowed us to noninvasively evaluate cortical sensory representations in rats, before and after injury. The FOV included both cortical hemispheres (Fig. 2*A–C*). Electrical stimulation (6 mA, 0.5 ms, 3 Hz for 40 s) of the forepaw or the hindpaw in intact animals resulted in a BOLD response in the contralateral sensory-motor cortex (Fig. 2*A*,*D*). We found that lower stimulation amplitudes resulted in activation of the same area in the sensory cortex (supplemental Fig. 3, available at www.jneurosci.org as supplemental material). Regardless of the stimulation strength used, activation of the somatosensory cortex was strictly contralateral. Electrical stimulation of the ipsilesional forepaw or hindpaw did not result in a BOLD response in either the ipsilateral or contralateral sensory-motor cortex both at 4 and 12 weeks after injury (data not shown).

Behavioral observations showed that the spared contralesional forelimb was used extensively after injury to compensate for the dysfunctional ipsilesional forelimb. This may lead to alterations of the corresponding forelimb representation in the ipsilesional cortex. Indeed, 4 weeks after injury, the sensory-motor cortical areas activated by stimulation of the contralesional forepaw were altered with large variations between animals, ranging from a 30% decrease to a 70% increase compared with an average map size in intact animals (Fig. 2*B*,*E*,*G*). Twelve weeks after injury, variations were smaller, and there was a significant 75% increase in the area activated by the forepaw stimulation (Fig. 2*G*). This expansion was mostly medial to the original forepaw representation with marginal expansions into the adjacent hindpaw field (Fig. 2*C*,*F*). The expansion at 12 weeks was accompanied by an increase in BOLD signal amplitude in response to the first stimulation train compared with normal rats (Fig. 2*H*). For subsequent stimulation trains, the responses got weaker. The amplitude reduction was more pronounced at 4 weeks after injury than at 12 weeks.

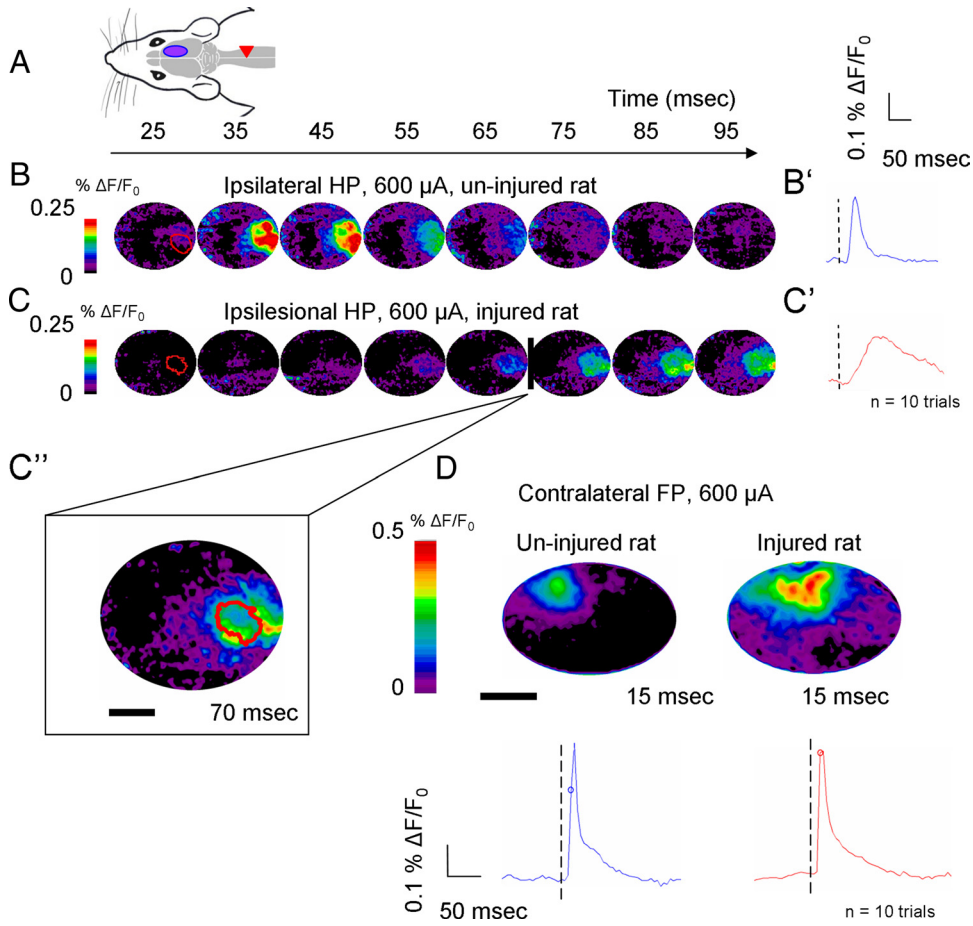

Figure 4. VSD imaging after stimulation of the ipsilesional hindpaw results in activation of the ipsilateral somatosensory cortex. ***A***, Scheme of the FOV with respect to the lesion (red arrowhead). ***B***, ***C***, Spatio-temporal dynamics of cortical activity in the ipsilesional cortex. Stimulation of the ipsilateral hindpaw in an intact animal (***B***) resulted in activation at short latency. The corresponding mean time activity curve with the hindpaw cortex as the ROI (***B′***; $n = 10$ trials). Twelve weeks after injury (***C***), the same stimulation led to a specific but delayed activation in the ipsilateral hindlimb cortex (time activity curve; ***C′***). The activation was specifically intense in the hindlimb field (***C″***). Red boundaries depict contralateral hindpaw activation field in the same animal. ***D***, Stimulation of the unimpaired forepaw resulted in a strong initial activation 12 weeks after injury. Ovals on the corresponding time activation curves show signal amplitude measured at 15 ms after stimulation (ROI, 70% isocentric contours 20 ms after forepaw stimulation). The vertical dashed line in ***C′***, ***B′***, and ***D*** depicts stimulation. Scale bars, 1.5 mm.

VSD imaging of cortical sensory-motor forepaw and hindpaw representations in intact rats

VSD imaging, which has a temporal resolution in the millisecond range, was used to characterize the spatio-temporal nature of the sensory-motor maps of the contralateral and ipsilateral limbs. In intact rats, a relatively weak electrical stimulation (600 μA, 1 pulse, 1 ms) of the forepaw resulted in a very localized activation of the contralateral sensory cortex starting 15 ms after stimulation (Fig. 3*B*,*B′*). In the following 10 ms, the site of activation moved medially into the forelimb motor cortex. Stimulation of the ipsilateral intact forepaw showed only a medial, presumably motor, activation that appeared slowly (25 ms) and was less intense than the contralateral stimulation (Fig. 3*C*,*C′*); over time (55 ms), a significant activation of the hindpaw field was also observed. In contrast to the forepaw stimulation, contralateral (Fig. 3*D*,*D′*) and ipsilateral (Fig. 3*E*,*E′*) hindpaw stimulation resulted in the activation of the same area. Again, contralateral paw stimulation triggered a faster (25 ms vs 43 ms latency to peak amplitude) and stronger response than ipsilateral stimulation; forepaw motor representation was also activated at a later time point (65 ms). Quantification of the response amplitude (Fig. 3*F*) and the latency to peak (Fig. 3*G*) from several animals ($n = 5$) confirmed the weak and slow response from ipsilateral limbs compared with the input from contralateral limbs.

VSD imaging shows cortical responses after ipsilesional hindpaw stimulation

Given the much higher sensitivity of VSD imaging, made evident by its ability to reveal ipsilateral sensory input that remained undetected by BOLD-fMRI, we were prompted to reexamine whether the ipsilesional (intact) cortex has assessed input from the injured side. As mentioned before, electrical stimulation of the forepaw in intact animals results in a significant activation of the contralateral sensory-motor and ipsilateral motor cortices. In injured animals, stimulation of the ipsilesional forepaw did not show any VSD response in the cortex ipsilateral to stimulation at 12 weeks after injury, and the FOV was not large enough to simultaneously observe the contralateral cortex. Stimulation of the hindpaw in intact rats results in a significant activation in the ipsilateral sensory-motor cortex within the first 60 ms (latency to peak, 43 ms) (Fig. 4*B*,*B′*); the activation was primarily confined to the hindpaw representation. At 12 weeks after injury, a significant activation of the ipsilateral hindpaw representation was seen (Fig. 4*C*,*C′*,*C″*). These responses occurred at much longer latencies in the injured group (at 100 ± 9 ms SEM after injury compared with 43 ± 3 ms SEM in intact animals; $p < 0.01$, Mann–Whitney *U* test; $n = 6$ rats).

We also stimulated the contralesional forepaw to reveal the underlying neural activity that led to the expansion of BOLD

activation maps after injury. At 15 ms after stimulation, the first time point at which VSD signal change is detected, the amplitude was ~1.7-fold higher in injured animals (Fig. 4*D*) (90.17 ± 0.02% $\Delta F/F_0$ SEM in intact animals and 0.30 ± 0.05% $\Delta F/F_0$ SEM after injury; $p < 0.05$, Mann–Whitney *U* test; $n = 5$ rats). This suggests that the BOLD expansion at 12 weeks after injury is attributable to increased neuronal activity in the forelimb sensory cortex evoked by electrical stimulation of the corresponding paw.

Increase of midline-crossing corticospinal axons from the intact CST after spinal cord injury

For the demonstrated ipsilesional hindpaw sensory input to be of relevance to the spontaneous behavioral recovery of the hindlimb, the intact cortex must have access to the denervated spinal cord. The CST originating in the ipsilesional cortex was labeled with the anterograde tracer BDA. The spinal cord contralateral to the injected cortex showed dense CST innervation of the dorsal and ventral horns in the examined cervical and lumbar segments in intact animals. There were very few midline-crossing axons in intact animals (Fig. 5*A*), and these were directed mostly toward the ventral horn in cervical segments (Fig. 5*B*,*D*) and toward the dorsal and ventral horn in lumbar segments (Fig. 5*C*,*E*). There was a large increase in midline-crossing CST axons 4 weeks after injury, over the dorsal and ventral commissure (Fig. 5*A*′–*C*′). In cervical segments (C5–C8), these midline-crossing axons preferentially projected toward the ventral horn (Fig. 5*B*′,*D*′), whereas in the lumbar segments (L2–L6) they projected dorsally and ventrally (Fig. 5*C*′,*E*′). Few branch points were observed in the axons that crossed the midline in intact and injured animals. The number of midline-crossing CST axons was quantified as intersections of three vertical lines placed on the gray matter; these lines were at 50 μm (M) and 240 μm (D1) from the midline in C5–C6 and L2–L6, and an additional line (D2) was placed at 560 μm in the cervical or 480 μm in the lumbar spinal cord. Normalized intersection counts in the cervical (Fig. 5*F*) or lumbar (Fig. 5*G*) spinal cord revealed a 6- to 10-fold increase in midline-crossing CST axons after injury.

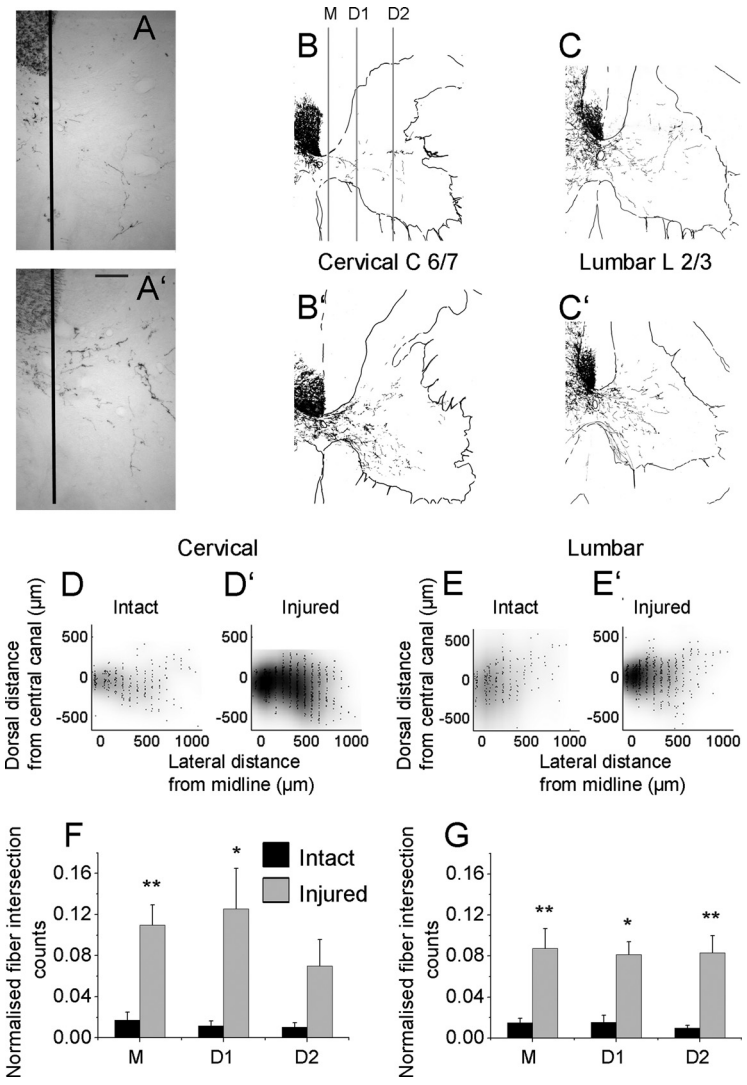

Figure 5. Increase of midline-crossing CST axons 4 weeks after unilateral cervical spinal cord injury. ***A–C***, BDA-labeled CST axons in intact animals rarely crossed the midline in the cervical (***A***, ***B***) or lumbar (***C***) spinal cord. Four weeks after injury, the number of midline-crossing axons increased (***A′–C′***). Scale bar, 200 μm. Camera lucida drawings of midline-crossing CST axons in the cervical (***B***, intact; ***B′***, injured) and lumbar (***C***, intact; ***C′***, injured) segments. ***D***, ***E***, Midline-crossing axon innervation maps, generated from midline-crossing axon intersection points on an array of equally spaced parallel vertical lines (80 μm apart; additional two lines placed 50 μm before and after the midline) placed through the entire ipsilateral gray matter. There is a maximum projection of 40 subsequent cross sections in cervical (***D***, intact; ***D′***, injured) and lumbar (***E***, intact; ***E′***, injured) segments. Intensity of the gray value represents the number of sections showing midline-crossing fibers in the same region. ***F***, ***G***, Quantification of axon counts at 50 μm (M), 240 μm (D1), and 480–560 μm (D2) from the central canal, normalized to efficiency of tracing, confirms the observed increase in innervation of the gray matter by the ipsilateral cortex in both cervical (***F***) and lumbar (***G***) segments. $n = 5$ rats. Statistics are as in previous figures.

Cortical localization of midline-crossing CST neurons

To localize the cells of origin of the midline-crossing, ipsilaterally projecting CST fibers, the retrograde tracer Fast Blue was injected unilaterally into the ipsilesional gray matter of the cervical segments C6/7 (Fig. 6*A*). In intact animals, a mean of 2640 cells (±520 SEM; $n = 4$) were found in the contralateral cortex (counts based on every third section). Retrograde-labeled cell counts reveal only one-tenth of the estimated number of corticospinal cells projecting to the lower cervical spinal cord (Schreyer and Jones, 1988). The labeled cells were distributed at various proportions through the sensory-motor cortex; 27% of the cells originated from the rostral forelimb area (RFA), fewer than 2% of the cells were found in the secondary somatosensory area (S-II) and the hindlimb area (excluding cells in the hindlimb-forelimb overlap region), and the bulk of cells originated from the caudal forelimb area (CFA) (Fig. 6*B*). A significant proportion (15%) of cells in the CFA originated from the region of overlap with forelimb–S1. In the ipsilateral cortex, a mean of 67 labeled cells (±17 SEM; $n = 4$) were found (Fig. 6*B*). A key feature of the normal ipsilateral representation (which arises, to a large extent, from

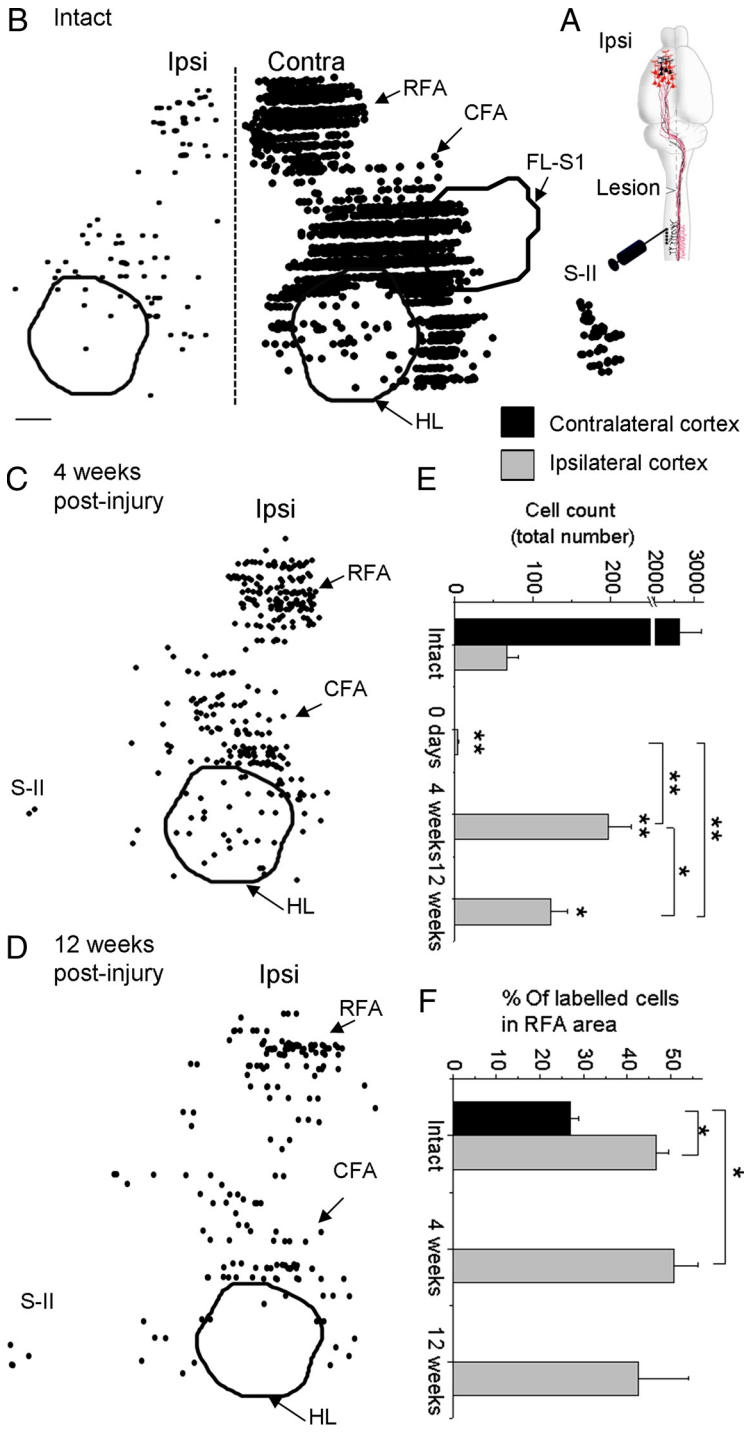

Figure 6. Retrograde localization of corticospinal neurons in the sensory-motor cortex reveals a new ipsilateral representation after lateral hemisection of the spinal cord. ***A***, Retrograde tracer was injected in the ipsilesional spinal cord below the lesion to label the cell bodies of midline-crossing fibers. ***B***, A dorsal view of the corticospinal representation in the contralateral and ipsilateral cortex. Each dot represents one labeled CST neuron. Representations were generated from cross sections through the cortex spaced at 100 μm. Scale bar, 500 μm. ***C***, ***D***, Ipsilateral CST representation 4 weeks (***C***) and 12 weeks (***D***) after injury. ***E***, Quantification of retrogradely labeled cortical CST cells ($n =$ 4 intact rats; $n = 5$ injury groups; counts from 50 μm brain sections with 100 μm gap). ***F***, Percentage of retrogradely labeled CST cells in the given hemisphere originating from the RFA area. Statistics are as in previous figures. Ipsi, ipsilesional; Contra, contralateral; FL-S1, primary forelimb sensory area; HL, hindlimb sensory-motor area (black boundary enclosed retrogradely labeled cut CST from lower thoracic spinal cord); RFA, rostral forelimb area; CFA, caudal forelimb area; S-II, secondary somatosensory area.

uncrossed axons in the pyramid) is the high proportion of cells in the RFA, which was almost twice that seen in the contralateral cortex (47% vs 27%). There were no cells in S-II, and fewer than 5% of the cells originated from the hindlimb area (exclusive of hindlimb–forelimb overlap region); the hindlimb area was determined by retrograde labeling of cut CST (in the dorsal funiculus) from the thoracic-8 segment in four independent experiments.

A unilateral hemisection injury disconnects the ipsilesional spinal cord from the cortex on the same side because of transection of the uncrossed CST. However, the preexisting midline-crossing CST axons remain. When the retrograde tracer was injected at the time of injury, a mean of only five cells (± 1 SEM; $n = 5$) were seen in the ipsilesional cortex. This confirms that in intact animals, only a minority of the ipsilateral cells project to the spinal cord gray matter by crossing at the segmental level and that the majority of the ipsilateral representation is attributable to the uncrossed CST axons. When traced 4 weeks after injury, the number of ipsilateral cells increased to 197 ($\pm$29 SEM; $n = 5$) (Fig. 6*E*). About half of these cells originated from the RFA, fewer than 10% of the cells originated from the hindlimb area, and some labeled cells were also found in S-II (Fig. 6*C*,*F*). At 12 weeks after injury, there was a significant decline in the number of cells (mean, 123 $\pm$ 22 SEM; $n = 5$) (Fig. 6*D*–*F*). The high percentage of cells originating from the RFA area and the low proportion of cells in S-II remained as observed at 4 weeks, whereas cells in the hindlimb area were absent. At both 4 and 12 weeks after injury, the labeled cells in the CFA originated medially, away from the forelimb–S1–CFA overlap region.

Discussion

The present results show that the intact (ipsilesional) adult rat sensory-motor cortex developed altered sensory input representations and corticospinal output projections after a unilateral spinal cord hemisection injury. Increased functional reliance on the unimpaired forelimb was accompanied by an expanded forelimb representation in the sensory cortex. The enhancement was observed using both BOLD-fMRI and VSD imaging. Using the highly sensitive VSD imaging technique, we also found that in uninjured animals, the cortex receives inputs from both ipsilateral forepaws and hindpaws. After injury, stimulation of the ipsilesional hindpaw, but not forepaw, induced a strong but delayed activation of the corresponding ipsilateral (intact) cortex. Sprouting of intact-side CST axons across the midline was observed in the lumbar and cervical spinal cord after C3/4 hemisection. The origin of the sprouting CST axons in the cervical cord was the ipsilateral CFA and RFA and the secondary sen-

sory area (S-II). The somatotopic similarity of the new ipsilateral corticospinal projection to the contralateral projection in intact animals suggests that new ipsilateral neurons may functionally compensate for the disconnected contralateral neurons.

Behavioral similarities of the rat injury model to Brown-Séquard syndrome in humans

Similarly to humans with well defined cervical unilateral hemisection injuries, the ipsilesional forelimb in our rats showed severe impairments with only negligible recovery of skilled movements (Taylor and Gleave, 1957). Ipsilesional hindlimbs recovered well for overground locomotion and partially in the ability to place the paw on the horizontal ladder rungs. During overground locomotion, ipsilesional forelimbs and hindlimbs showed nearly complete recovery of rhythmicity; the body weight supported by the forelimb was, however, less than in the intact situation. Patients with Brown-Séquard syndrome often regain their ability to walk, with minimal external support, after lesions at either cervical (Taylor and Gleave, 1957; Roth et al., 1991) or thoracic (Little and Halar, 1985) spinal segments. These similarities validated the cervical lateral hemisection injury in rodents as a model for understanding Brown-Séquard syndrome in humans.

The deficits in skilled walking of the ipsilesional forelimb, ipsilesional hindlimb, and even the contralesional hindlimb may be partly attributable to severed propriospinal circuits that make coordinated quadrupedal locomotion possible (Metz and Whishaw, 2002; Juvin et al., 2005). A stronger descending influence on the forelimb compared with the hindlimb may play a crucial role in keeping the contralesional forelimb placements error free.

Increase in size of sensory activation map of the unimpaired forepaw after injury

We applied subcutaneous electrical stimulation at the forepaw or hindpaw to elicit neuronal responses in the sensory cortex. A current of 6 mA presumably activates tactile and proprioceptive, but not nociceptive, pathways in the sensory cortex (Shih et al., 2009). The cortical BOLD response to painful stimulation is bilateral, and in our study, the BOLD responses were strictly contralateral to the side of stimulation (Shih et al., 2008a,b). Nevertheless, exactly which sensory modalities were activated by the stimulation used (6 mA) in our BOLD-fMRI experiments remains contentious. This is less so in VSD imaging since a current amplitude of 600 μA could be used, which is much lower than the speculated nociceptive threshold.

BOLD-fMRI mapping of the contralesional forepaw representation in the intact cortex showed a marked increase in size 12 weeks after injury. This expansion was seen mainly into regions medial to the original forepaw representation; these include the forepaw motor area. Forepaw and hindpaw representations remained well separated, however. The expansion into the motor area suggests increased sensory-motor interactions, perhaps because of strengthened horizontal cortical connections (Rioult-Pedotti et al., 1998). VSD imaging, which detects subthreshold and suprathreshold membrane potential changes of the superficial cortical layers, likewise revealed stronger activation of the forelimb sensory cortcex after contralesional forepaw stimulation 12 weeks after C3 hemisection. These alterations may be driven by acquisitions of new movements or movement strategies after injury, and not just repetitive use (Nudo, 2006).

New ipsilesional hindlimb input to the intact cortex after injury

In uninjured animals used for VSD experiments, the responses in the sensory-motor cortex ipsilateral to the stimulated forepaw or hindpaw were weak and had longer latencies than in the contralateral cortex. The contralateral paw activated both sensory (at 15 ms after stimulation) and motor (within the next 10 ms) regions, whereas the ipsilateral paw primarily activated the forepaw motor cortex (at 25–35 ms). In the hindlimb field, such a spatial distinction was not possible as the sensory and motor representations overlap completely (Donoghue and Wise, 1982). The ipsilateral sensory input, which is presumably transmitted transcallosally, has been previously suggested to provide inhibition to the sensory cortex as revealed by the lack of significant activation in the sensory cortex in response to ipsilateral forelimb stimulation (Calford, 2002). However, the strong activation of the forelimb motor area suggests a larger role of ipsilateral sensory inputs in motor function. In humans, ipsilateral input has been suggested to modulate corticospinal excitability and complex finger movements (Chen et al., 1997).

Electrical stimulation of the ipsilesional hindpaw at 600 μA in spinal cord-injured rats resulted in a specific activation of the hindlimb cortex. This activation was, however, delayed compared with the ipsilateral activation in uninjured animals. How does the sensory information from the ispilesional hindpaw reach the ipsilateral (intact) cortex in the absence of functional dorsal column pathways? One possible explanation could be via the spino-thalamic tract (STT). The cell bodies of the STT lie in the spinal cord dorsal horn and their axons project across the midline to relay sensations to the contralateral somatosensory cortex somatotopically (Schouenborg et al., 1986). Notably, in rat lumbar cord, ~30% of the STT cells respond exclusively to non-noxious stimulation (Giesler et al., 1976). Whether the delayed activation of the ipsilesional sensory-motor cortex observed here 12 weeks after injury transmits mechano-sensory sensation remains to be determined.

CST axons of the intact side sprout across the spinal cord midline in a region-specific manner

Unilateral anterograde labeling of the CST in uninjured adult rats showed few rare axons crossing the midline to innervate the ipsilateral spinal cord. After injury, however, the number of midline-crossing axons increased ~6- to 10-fold at both cervical and lumbar levels; the tracer was applied to the entire motor cortex. The CST from the forelimb cortex does not project to lumbar segments; these segments are innervated exclusively by axons originating in the hindlimb cortex (Akintunde and Buxton, 1992). Therefore, it is safe to assume that the midline-crossing axons seen in the lumbar segments originate from the hindlimb cortex. The increase in midline-crossing fibers in the cervical segments after injury correlated with a higher number of retrogradely labeled ipsilateral cells in the forelimb motor cortex. Interestingly, midline-crossing axons in cervical segments projected predominantly toward the ventral horn. This suggests their origin in the motor rather than the sensory cortex (Kuang and Kalil, 1990; Bareyre et al., 2002). A motor bias of the midline-crossing CST is also demonstrated by the high proportion of neurons that originated from the RFA, which is suggested to be primarily motor (Neafsey and Sievert, 1982; Sanderson et al., 1984; Rouiller et al., 1993).

Does the intact cortex influence the ipsilesional side via the midline-crossing corticospinal neurons? In the lumbar spinal cord, the midline-crossing fibers have access to sensory inputs

from the ipsilesional hindlimb as suggested by our VSD imaging results discussed above. The partial recovery of skilled placement by the ipsilesional hindpaw may be driven by this new ipsilateral circuitry. The lack of recovery of the ipsilesional forelimb in skilled walking may be partly caused by the absence of sensory inputs from this paw to the intact (ipsilesional) cortex from which the new corticospinal representation originates. The sensory inputs may also play a crucial role by sustaining cortical neuronal activity and therefore in maintaining hindlimb motor intracortical circuits (Chakrabarty and Martin, 2005). Improvement in limb placements during overground locomotion by both ipsilesional forelimbs and hindlimbs too may be driven by cortical plasticity. In the neonatally spinalized rats, sensorimotor cortex reorganizes to participate in overground locomotion (Giszter et al., 2008); in intact rats, the cortex is thought to have little role in this form of locomotion.

In conclusion, the ipsilesional sensory and motor cortices undergo important reorganizations that parallel both increased compensatory usage on the unimpaired side and the partial functional recovery of the impaired limbs. The sensory-motor alterations on the injured side result in a new ipsilateral cortico-spinal circuitry that could reflect a side-switch in the cortical control of the denervated spinal cord.

References

Akintunde A, Buxton DF (1992) Differential sites of origin and collateralization of corticospinal neurons in the rat: a multiple fluorescent retrograde tracer study. Brain Res 575:86–92.

Bareyre FM, Haudenschild B, Schwab ME (2002) Long-lasting sprouting and gene expression changes induced by the monoclonal antibody IN-1 in the adult spinal cord. J Neurosci 22:7097–7110.

Bolton DA, Tse AD, Ballermann M, Misiaszek JE, Fouad K (2006) Task specific adaptations in rat locomotion: runway versus horizontal ladder. Behav Brain Res 168:272–279.

Brown-Séquard CE (1868) Lectures on the physiology and pathology of the nervous system; and on the treatment of organic nervous affections. Lancet 92:593.

Bruehlmeier M, Dietz V, Leenders KL, Roelcke U, Missimer J, Curt A (1998) How does the human brain deal with a spinal cord injury? Eur J Neurosci 10:3918–3922.

Brus-Ramer M, Carmel JB, Chakrabarty S, Martin JH (2007) Electrical stimulation of spared corticospinal axons augments connections with ipsilateral spinal motor circuits after injury. J Neurosci 27:13793–13801.

Calford MB (2002) Dynamic representational plasticity in sensory cortex. Neuroscience 111:709–738.

Chakrabarty S, Martin JH (2005) Motor but not sensory representation in motor cortex depends on postsynaptic activity during development and in maturity. J Neurophysiol 94:3192–3198.

Chen R, Gerloff C, Hallett M, Cohen LG (1997) Involvement of the ipsilateral motor cortex in finger movements of different complexities. Ann Neurol 41:247–254.

Donoghue JP, Wise SP (1982) The motor cortex of the rat: cytoarchitecture and microstimulation mapping. J Comp Neurol 212:76–88.

Endo T, Spenger C, Tominaga T, Brene S, Olson L (2007) Cortical sensory map rearrangement after spinal cord injury: fMRI responses linked to Nogo signalling. Brain 130:2951–2961.

Ferezou I, Haiss F, Gentet LJ, Aronoff R, Weber B, Petersen CC (2007) Spatiotemporal dynamics of cortical sensorimotor integration in behaving mice. Neuron 56:907–923.

Giesler GJ, Menetrey D, Guilbaud G, Besson JM (1976) Lumbar cord neurons at the origin of the spinothalamic tract in the rat. Brain Res 118:320–324.

Giszter S, Davies MR, Ramakrishnan A, Udoekwere UI, Kargo WJ (2008) Trunk sensorimotor cortex is essential for autonomous weight-supported locomotion in adult rats spinalized as P1/P2 neonates. J Neurophysiol 100:839–851.

Hamers FP, Koopmans GC, Joosten EA (2006) CatWalk-assisted gait analysis in the assessment of spinal cord injury. J Neurotrauma 23:537–548.

Juvin L, Simmers J, Morin D (2005) Propriospinal circuitry underlying interlimb coordination in mammalian quadrupedal locomotion. J Neurosci 25:6025–6035.

Kaas JH, Qi HX, Burish MJ, Gharbawie OA, Onifer SM, Massey JM (2008) Cortical and subcortical plasticity in the brains of humans, primates, and rats after damage to sensory afferents in the dorsal columns of the spinal cord. Exp Neurol 209:407–416.

Kartje-Tillotson G, O'Donoghue DL, Dauzvardis MF, Castro AJ (1987) Pyramidotomy abolishes the abnormal movements evoked by intracortical microstimulation in adult rats that sustained neonatal cortical lesions. Brain Res 415:172–177.

Kuang RZ, Kalil K (1990) Specificity of corticospinal axon arbors sprouting into denervated contralateral spinal cord. J Comp Neurol 302:461–472.

Little JW, Halar E (1985) Temporal course of motor recovery after Brown-Sequard spinal cord injuries. Paraplegia 23:39–46.

Metz GA, Whishaw IQ (2002) Cortical and subcortical lesions impair skilled walking in the ladder rung walking test: a new task to evaluate fore- and hindlimb stepping, placing, and co-ordination. J Neurosci Methods 115:169–179.

Neafsey EJ, Sievert C (1982) A second forelimb motor area exists in rat frontal cortex. Brain Res 232:151–156.

Nudo RJ (2006) Plasticity. NeuroRx 3:420–427.

Raineteau O, Schwab ME (2001) Plasticity of motor systems after incomplete spinal cord injury. Nat Rev Neurosci 2:263–273.

Rioult-Pedotti MS, Friedman D, Hess G, Donoghue JP (1998) Strengthening of horizontal cortical connections following skill learning. Nat Neurosci 1:230–234.

Roth EJ, Park T, Pang T, Yarkony GM, Lee MY (1991) Traumatic cervical Brown-Sequard and Brown-Sequard-plus syndromes: the spectrum of presentations and outcomes. Paraplegia 29:582–589.

Rouiller EM, Moret V, Liang F (1993) Comparison of the connectional properties of the two forelimb areas of the rat sensorimotor cortex: support for the presence of a premotor or supplementary motor cortical area. Somatosens Mot Res 10:269–289.

Sanderson KJ, Welker W, Shambes GM (1984) Reevaluation of motor cortex and of sensorimotor overlap in cerebral cortex of albino rats. Brain Res 292:251–260.

Schouenborg J, Kalliomaki J, Gustavsson P, Rosen I (1986) Field potentials evoked in rat primary somatosensory cortex (SI) by impulses in cutaneous A beta- and C-fibres. Brain Res 397:86–92.

Schreyer DJ, Jones EG (1988) Axon elimination in the developing corticospinal tract of the rat. Brain Res 466:103–119.

Shih YY, Chen YY, Chen CC, Chen JC, Chang C, Jaw FS (2008a) Whole-brain functional magnetic resonance imaging mapping of acute nociceptive responses induced by formalin in rats using atlas registration-based event-related analysis. J Neurosci Res 86:1801–1811.

Shih YY, Chang C, Chen JC, Jaw FS (2008b) BOLD fMRI mapping of brain responses to nociceptive stimuli in rats under ketamine anesthesia. Med Eng Phys 30:953–958.

Shih YY, Chen CC, Shyu BC, Lin ZJ, Chiang YC, Jaw FS, Chen YY, Chang C (2009) A new scenario for negative functional magnetic resonance imaging signals: endogenous neurotransmission. J Neurosci 29:3036–3044.

Sydekum E, Baltes C, Ghosh A, Mueggler T, Schwab ME, Rudin M (2009) Functional reorganization in rat somatosensory cortex assessed by fMRI: elastic image registration based on structural landmarks in fMRI images and application to spinal cord injured rats. Neuroimage 44:1345–1354.

Tattersall R, Turner B (2000) Brown-Sequard and his syndrome. Lancet 356:61–63.

Taylor RG, Gleave JR (1957) Incomplete spinal cord injuries; with Brown-Sequard phenomena. J Bone Joint Surg Br 39-B:438–450.

Thallmair M, Metz GA, Z'Graggen WJ, Raineteau O, Kartje GL, Schwab ME (1998) Neurite growth inhibitors restrict plasticity and functional recovery following corticospinal tract lesions. Nat Neurosci 1:124–131.

Wiessner C, Bareyre FM, Allegrini PR, Mir AK, Frentzel S, Zurini M, Schnell L, Oertle T, Schwab ME (2003) Anti-Nogo-A antibody infusion 24 hours after experimental stroke improved behavioral outcome and corticospinal plasticity in normotensive and spontaneously hypertensive rats. J Cereb Blood Flow Metab 23:154–165.

Zhou L, Shine HD (2003) Neurotrophic factors expressed in both cortex and spinal cord induce axonal plasticity after spinal cord injury. J Neurosci Res 74:221–226.